Experimental and kinetic modeling study of the pyrolysis and oxidation of 1,5-hexadiene: The reactivity of allylic radicals and their role in the formation of aromatics

Florence H. Vermeire[1], Ruben De Bruycker[1], Olivier Herbinet[2], Hans-Heinrich Carstensen[1], Frédérique Battin-Leclerc[2], Guy B. Marin[1], .Kevin M. Van Geem[1],*

[1] Laboratory for Chemical Technology, Ghent University, Technologiepark 914, 9052 Gent, Belgium

[2] Laboratoire Réactions et Génie des Procédés, CNRS, Université de Lorraine, Nancy, France

Published in Fuel, 2017, 208, 779-790

Highlights

- New experimental datasets for 1,5-hexadiene pyrolysis and oxidation at 500–1100 K.
- Detailed kinetic model predicts experimental mole fractions including aromatics well.
- Different pathways for the formation of cyclopentadiene and aromatics are discussed.
- Identification of sensitive reactions for fuel conversion and aromatics formation.

Abstract

Resonantly stabilized radicals play an important role in the formation of aromatics. In this work, the pyrolysis ($\varphi = \infty$) and oxidation ($\varphi = 1$ and 2) of 1,5-hexadiene, diluted in He, has been studied experimentally in a jet-stirred reactor at atmospheric pressure. The temperature was varied between 500 and 1100 K and the residence time was fixed at 2 s. Gas chromatography was used to determine the reactor effluent composition. The dedicated analysis section allowed the identification and quantification of many hydrocarbon and oxygenated product species up to naphthalene. The pyrolysis of 1,5-hexadiene results in the formation of small alkenes and cyclic hydrocarbons, with a particularly high selectivity towards 1,3-cyclopentadiene and benzene. In the presence of molecular

oxygen, various oxygenated intermediates, including acrolein, prop-2-en-1-ol and but-3-enyl-oxirane, were detected in the outlet gases, besides the pyrolysis products. A detailed kinetic model was developed, mainly with an automatic network generation tool, to simulate and interpret the performed experiments. The kinetic model includes molecular weight growth chemistry to predict mole fractions of the main aromatic species. Model calculated and experimental mole fraction profiles are in relatively good agreement. At low-temperature pyrolysis conditions, 1,5-hexadiene is in quasi-equilibrium with allyl radicals. Hydrogen abstraction from 1,5-hexadiene by allyl radicals has the strongest effect on conversion. The resulting hexa-2,5-dien-1-yl radical can react by intramolecular radical addition and eventually form 1,3-cyclopentadiene and benzene. Recombination of cyclopentadienyl with alkyl radicals followed by hydrogen abstraction and ring enlargement is an important formation path to aromatics. At oxidizing conditions, the pyrolysis reaction pathways are in competition with reactions involving hydroxyl and hydroperoxy radicals, as well as molecular oxygen. Above 900 K, 1,5-hexadiene is mainly consumed by C-C scission. The conversion and product distribution in 1,5-hexadiene oxidation are found to be sensitive to the branching ration of the reactions of allyl with hydroperoxy radicals. Formation of hydroxyl and allyloxy radicals increases the reactivity while the propene and molecular oxygen channel decreases the number of radicals in the system.

Keywords: 1, 5-Hexadiene, Allyl, Jet-stirred reactor, Recombination reactions, Aromatics formation

1. Introduction

The pyrolysis and oxidation of hydrocarbon and oxygenated molecules often lead to the formation of polycyclic aromatic hydrocarbons (PAH) which are considered the main precursors for deposits or soot particles [1]. Resonantly stabilized radicals, such as propargyl, allyl and cyclopentadienyl, have been identified as important intermediates for PAH formation [2–5]. They have prolonged lifetimes compared to non-resonantly stabilized radicals and therefore accumulate at fuel-rich oxidation or pyrolysis conditions. Recombination with other radicals in the reactive system is an important consumption route leading to molecular weight growth [6]. In this respect, the self-recombination of propargyl radicals to benzene has been investigated thoroughly [5,7,8]. Other recombination channel routes that eventually lead to benzene include allyl plus propargyl, allyl plus allyl and cyclopentadienyl plus methyl radicals and addition of vinyl to 1,3-butadiene [2,6,9,10]. The relative importance of each benzene formation path depends on the operating conditions and the molecular structure of the feed molecule. For example, a significant proportion of benzene is formed in 1-alkene flames by the recombination of allyl with propargyl radicals via fulvene [2,11–13]. The recombination of allyl radicals has been identified as a significant reaction path during the pyrolysis (<1200 K) of molecules with a high selectivity towards allyl radicals [6,14,15].

The self-recombination of allyl radicals results in the formation of 1,5-hexadiene, which upon hydrogen abstraction from the allylic carbon atoms forms hexa-2,5-dien-1-yl radicals. Cyclization of hexa-2,5-dien-1-yl radicals produces C_5 and C_6 ring species [16,17]. Note that hexa-2,5-dien-1-yl radicals are also formed by vinyl addition to 1,3-butadiene [13].

The reactions of allyl radicals obtained via 1,5-hexadiene formed via 1,5-hexadiene decomposition have been studied before. In 1960, Ruzicka et al. [18] pyrolysed 1,5-hexadiene in a quartz vessel at 9.3 kPa between 733 K and 794 K at various reaction times. A mechanism was proposed based on hydrogen abstraction reactions by allyl radicals and addition of allyl radicals to double bonds. Golden et al. [19] reported in 1969 the direct measurement of the equilibrium coefficient at 913 K and 1063 K for the reaction between two allyl radicals and 1,5-hexadiene. Homer et al. [20] did experiments with very low helium carrier gas pressures (1.3–6.7 kPa) between 977 K and 1070 K in a flow type reactor coupled to a mass spectrometer, to investigate the scission reaction without the interference of secondary reactions. Pyrolysis experiments in a stirred-flow type reactor with toluene carrier flow between 850 K and 950 K at low pressures (1.6–2.3 kPa) were conducted by Akers et al. in 1967 [21].

Three competing pathways for the consumption of allyl radicals were proposed, i.e. recombination back to 1,5-hexadiene, hydrogen abstraction reaction from toluene and recombination with a benzyl radical. In 1973, Nohara et al. [22] performed experiments in a flow-type apparatus between 773 K and 893 K with nitrogen dilution at atmospheric pressure. A new reaction scheme was proposed with elementary reactions that focus on the formation of C_5 products. McDonald et al. [23] studied the cyclic products formed from 1,5-hexadiene by continuous wave CO_2 laser-induced experiments at low pressures. More recently, in 2005, Isemer et al. [24] determined rate expressions for the self-reaction of allyl radicals and the reactions between allyl radicals and acetylene, hydrogen gas and methane in shock tube experiments for temperatures between 1000 K and 1400 K. Additional measurements of the allyl radical recombination rate coefficient using the pulsed-laser photolysis/cavity ring-down spectroscopy technique have been reported by Matsugi et al. [25], new shock tube results have been published by Fridlyand et al. [26] and theoretical calculations for this reaction are done by Georgievskii et al. [27].

Further insight in the oxidation chemistry of hexadiene isomers is provided by McEnally et al. [28] who studied non-premixed 2D methane flames doped with hexadiene isomers. The focus of this research was on the role of hexadienes in high temperature soot formation. In 2010, a detailed kinetic model was developed by Sharma et al. [17] to study the chemistry of 1,3-hexadiene and 1,4-hexadiene in these flames. They concluded that recombination of methyl and propargyl radicals with cyclopentadienyl are important formation pathways for benzene and styrene respectively.

The reactivity of allyl radicals is also of importance during the oxidation and pyrolysis of propene. The oxidation of propene has been thoroughly studied experimentally and the results have been used by Burke et al. [29,30] to develop a well-validated oxidation model. Wang et al. [6] have developed a fundamentally-based kinetic model to characterize the molecular weight growth during propene pyrolysis.

The current work addresses the lack of comprehensive experimental data sets for 1,5-hexadiene pyrolysis and oxidation conditions in a jet-stirred reactor at low to intermediate temperatures. This is motivated by the interest to understand the role that 1,5-hexadiene and allylic radicals play in the formation of aromatics within the primary decomposition chemistry. Therefore In this work, hydrocarbon and oxygenated product species up to naphthalene have been identified and quantified. In order to interpret the data, a detailed kinetic model has been developed using an automatic

network generation tool. This model was augmented with kinetic data from several recent literature-reported theoretical calculations. The model is able to predict the trend of the main product species, including aromatics, well. The reaction pathways responsible for the formation of the main product species, 1,3-cyclopentadiene and aromatics have been identified by rate of production and sensitivity analyses.

2. Experimental methods

The applied experimental setup is an isothermal quartz jet-stirred reactor with a dedicated feed section and analysis section for outlet gases. The main features of the apparatus are discussed below, details can be found elsewhere [31,32].

Helium and oxygen were provided by Messer (purities of 99.99% and 99.999% respectively) while 1,5-hexadiene was provided by Sigma-Aldrich (purity of 98%). The helium and oxygen flow rates to the reactor are controlled with two gas-mass-flow controllers (Bronkhorst). The 1,5-hexadiene flow rate is regulated using a liquid-Coriolis-flow controller (Bronkhorst). The liquid is mixed with helium and passes through an evaporator (kept at 450 K). Afterwards, in oxidation experiments, oxygen is added to the gaseous flow.

The gaseous mixture flows through an annular preheating zone, where it is heated to the reactor temperature, and enters the jet-stirred reactor through four nozzles. The nozzles and reactor are designed to avoid thermal and concentration gradients. Thermocoax resistance wires provide heating for the annular preheating zone and the reactor. A type K thermocouple measures the temperature in the center of the reactor (measured temperature gradients <5 K). The pressure is set with a needle valve downstream of the reactor.

The exit of the reactor is connected to several gas chromatographs through heated transfer lines, kept at 473 K, to avoid condensation. The reactor effluent composition is quantified using three gas chromatographs. Response factors were determined by injecting known amounts of pure substances or using the effective carbon number method. The first gas chromatograph is equipped with a thermal conductivity detector and uses a Carbosphere packed column for separation. The second gas chromatograph has a flame-ionization detector, preceded by a methanizer, and is equipped with a PlotQ capillary column. The third gas chromatograph is equipped with a flame-ionization detector

and a HP-5MS capillary column. A forth gas chromatograph, which is used for product identification only, uses a PlotQ or HP-5MS capillary column for separation and a quadrupole mass spectrometer as detector.

In this work, the 1,5-hexadiene inlet mole fraction was kept constant at 0.008 and the total inlet volumetric flow rate at reactor temperature and pressure was fixed at 4.06 10^{-5} m^3 s^{-1}, which corresponds to a residence time of 2 s. Three equivalence ratios were investigated, i.e. $\varphi = 1.0$, 2.0 and ∞, for which the effluent compositions were quantitatively analyzed. The pressure was fixed at 0.107 MPa for all experiments and the reactor temperature was varied between 500 and 1100 K. The experimental procedure allowed to close the carbon molar balance within 5%. The hydrogen molar balance closed within 5% at pyrolysis conditions. Since water was not quantified in this work, hydrogen and oxygen molar balances could not be verified at $\varphi = 1.0$ and 2.0. The relative uncertainty on experimental mole fractions is approximately 5% for species that are calibrated using standards and 10% for species that are calibrated with the effective carbon number method. These uncertainty ranges are based on prior studies and account for repeatability errors, ambiguities in peak areas integration and inaccuracies of the effective carbon number [31,33,34].

3. Kinetic model development

A kinetic model has been developed for the oxidation and pyrolysis of 1,5-hexadiene, consisting of two parts. The first part is a submechanism containing reactions describing the consumption of 1,5-hexadiene and derived radicals. The second part of the developed kinetic model describes the pyrolysis and oxidation of propene, 1,3-cyclopentadiene and aromatics. The complete kinetic model, in CHEMKIN [35] format, is provided in Supplementary Data.

3.1. Submechanism for the pyrolysis and oxidation of 1,5-hexadiene

The majority of the 1,5-hexadiene submechanism has been generated automatically using Genesys [36,37]. After model generation, several key reactions and associated thermochemical data were replaced with literature-reported quantum chemical calculations and experimental observations.

3.1.1. Kinetic model construction

Genesys requires a set of initial molecules, i.e. reactants, and a set of reaction families as input. Each reaction family describes how reactants are transformed into products through the course of that specific reaction. For each reaction of a specific reaction family, Genesys assigns reaction rate coefficients using a methodology provided by the user, e.g. Evans-Polanyi relationships, group additivity for pre-exponential factors and activation energies, reactivity-structure-based rate rules or simple analogy with similar reactions. Thermochemical data for generated molecules and radicals are taken from extensive databases whenever possible [38,39]. Otherwise, Benson's group additivity concept for thermochemistry is used [40]. The algorithm in Genesys starts by reacting the initial molecules using the considered reaction families. The generated reactions and species are added to the reaction network. The algorithm continues until all generated species have reacted according to the provided reaction families. The user can add constraints to reaction families to prevent the generation of kinetically insignificant reactions.

3.1.2. Reaction families

The reaction families considered in the automated mechanism development step are listed below and more details are given in Supplementary Data.

The rate coefficients for the C-C and C-H β-scission reactions were calculated with the group additive method framework for pre-exponential factors and activation energies developed by Saeys [41] and Sabbe et al. [42,43]. Also for hydrogen abstraction reactions by hydrogen atoms and carbon-centered radicals, group additive values for Arrhenius parameters were used as calculated by Sabbe et al. [44]. Since no group additive database is available for hydrogen abstraction reactions by hydroxyl and hydroperoxy radicals from carbon atoms are currently available, these rate coefficients were estimated from analogous hydrogen abstraction reactions from alkanes and alkenes [45–48].

Kinetic parameters for intramolecular radical addition and hydrogen abstraction reactions were estimated using reactivity-structure-based estimation rules [49]. These reactions proceed through a cyclic transition state. The pre-exponential factor is correlated with the number of hindered rotors in the transition state and the activation energy is the sum of analogous bimolecular reaction and the ring strain in the transition state.

The reaction rate coefficients for addition reactions of molecular oxygen to carbon-centered radicals and subsequent reactions were estimated from analogous alkane and alkene reactions [50,51]. The reaction rate coefficient for the allyl plus hydroperoxy radicals reaction system [52] was used to estimate the recombination of hydroperoxy radicals with resonantly stabilized radicals and the subsequent decomposition of the hydroperoxide. These reactions were shown to be important in the oxidation of propene and 2-methyl-2-butene [29,53].

3.1.3. Updated C_6H_{10}, C_6H_9, C_6H_8, C_6H_6 and C_7H_{11} chemistry

After model generation, several reaction rate coefficients of key reactions and the associated thermochemical data of several species were replaced with literature-reported quantum chemical calculations and experimental observations. For example, the unimolecular decomposition of 1,5-hexadiene to allyl plus allyl radicals has recently been investigated in a shock tube [26,54]. The recommended kinetic and thermodynamic data were incorporated in the developed kinetic model. Wang et al. [16] investigated the reactivity of allylic radicals and calculated the C_6H_9 potential energy surface, which includes decomposition routes of hexa-2,5-dien-1-yl, and the C_7H_{11} potential energy surface that contains the addition of the allyl radical on 1,3-butadiene, at the CBS-QB3 level of theory [16]. The proposed high-pressure reaction rate coefficients were implemented in the kinetic model. Reaction rate coefficients for the self-reaction of propargyl and reaction of propargyl with allyl radicals were taken from Miller and coworkers [7,55,56].

3.2. Pyrolysis and oxidation of propene, 1,3-cyclopentadiene and aromatics

Propene, 1,3-cyclopentadiene and aromatics are important products in the oxidation and pyrolysis of 1,5-hexadiene and consumption pathways for these species need to be included for an adequate performance of the kinetic model. Therefore, the thoroughly validated propene oxidation model by Burke et al. [29,30] was added to the1,5-hexadiene submechanism to describe the propene chemistry. This model was extended with thermodynamic data determined by Goldsmith et al. [52] for important species formed during the reaction of an allyl radical with a hydroperoxy radical. The subsequent chemistry of 1,3-cyclopentadiene was taken from Green and coworkers [17,57]. Finally, submechanisms for the oxidation of aromatics, including benzene/toluene/styrene, were taken from Herbinet et al.[58].

4. Results and discussion

4.1. Experimental and modeling results

Experiments were performed at pyrolysis and oxidation conditions. Three equivalence ratios were studied, i.e. $\varphi = 1.0$, $\varphi = 2.0$ and $\varphi = \infty$. No "negative temperature coefficient" zone, in which the reactivity decreases with increasing temperature, was observed in the oxidation experiments. Alkenes are known to have reduced low-temperature reactivity compared to alkanes [59,60]. Hexa-2,5-dien-1-yl, the radical formed following hydrogen abstraction from the allylic carbon atom in 1,5-hexadiene, is resonantly stabilized. The resonance stabilization is lost upon addition of molecular oxygen. Redissociation of the adduct to the reactants is likely to be the major reaction path, rather than intramolecular hydrogen abstraction, which can trigger chain branching and low-temperature reactivity [59].

Sixty products were detected and quantified in the reactor outlet gases. Mole fraction profiles of all species as function of reactor temperature are reported in Supplementary Data. A selection of mole fraction profiles are displayed in Figure 1 ($\varphi = \infty$), Figure 2 ($\varphi = 1.0$) and Figure 3 ($\varphi = 2.0$). These species were chosen because they (a) have high yields during 1,5-hexadiene pyrolysis and oxidation, (b) are important intermediates of 1,5-hexadiene decomposition and/or (c) are PAH precursors.

The pyrolysis of 1,5-hexadiene results in the formation of small alkenes and a wide variety of cyclic hydrocarbons, such as cyclohexene, cyclohexadiene, 1,3-cyclopentadiene, methyl-cyclopentadiene, benzene and larger aromatics. The small unsaturated hydrocarbons, that are often found to be PAH precursors, with the highest mole fractions are ethene, ethyne, propene, propadiene, propyne, 1-butene and 1,3-butadiene.

The same products are also detected in the oxidation of 1,5-hexadiene, though their yields are generally lower and decrease with increasing oxygen content. Furthermore, several oxygenated species were identified. Acrolein, prop-2-en-1-ol, but-3-enyl-oxirane, acetaldehyde and formaldehyde were detected in relatively high quantities which can be attributed to several fuel decomposition channels as will be discussed in section 4.2. No ethenol was detected during the analysis, while this species is predicted to be formed in relatively high amounts. Ethanol is probably

completely converted to acetaldehyde downstream of the reactor and detected by the GC together with the acetaldehyde peak.

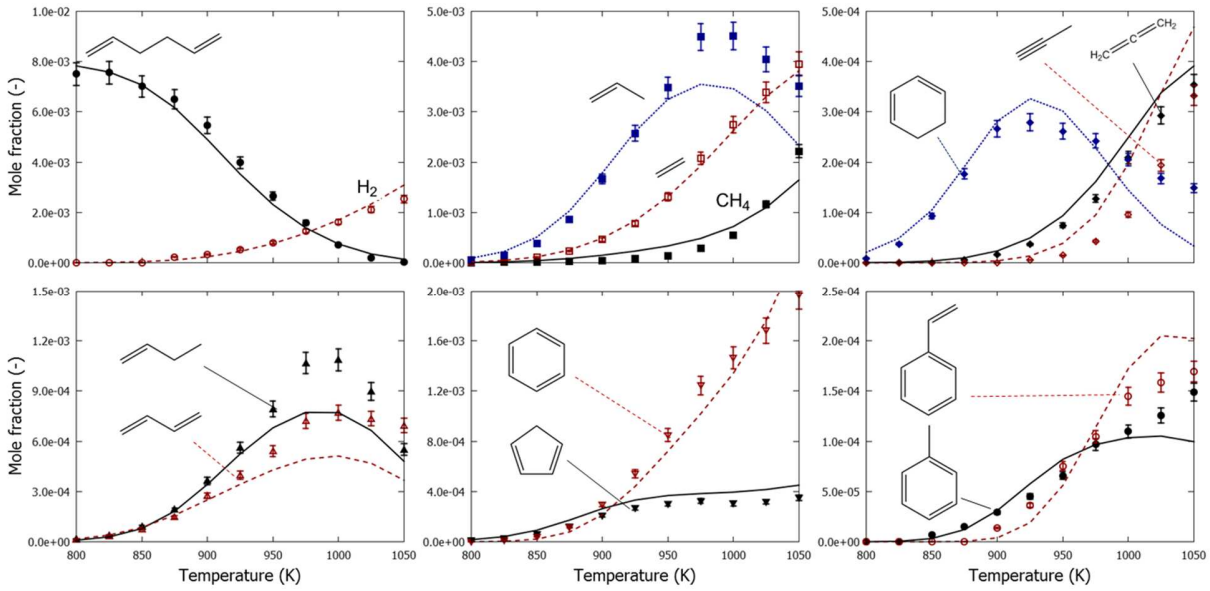

Figure 1: Mole fractions as function of temperature for 1,5-hexadiene pyrolysis ($\varphi = \infty$) in a jet-stirred reactor, P = 0.107 MPa, FV = 4.06 10^{-5} m^3 s^{-1}, $x_{1,5-hexadiene}^{inlet} = 0.008$: symbols, experimental mole fraction profile of molecule represented in graph; lines, mole fraction profiles calculated with CHEMKIN using the perfectly stirred reactor model and the developed kinetic model.

Reactor simulations were performed using the perfectly-stirred reactor module in CHEMKIN-PRO [35] and the developed kinetic model. Model calculated mole fraction profiles are included in Figures 1–3. The developed kinetic model is in qualitative agreement with most experimental data, i.e. the effect of temperature and equivalence ratio on mole fraction is accurately reproduced. For pyrolysis, the major products are also in quantitative agreement, as can be observed in Figure 1. The deviations between experimental and model calculated mole fractions are overall larger in oxidation conditions. Relative large discrepancies are observed for ethene, acrolein and acetaldehyde. These differences are further discussed in sections 4.2 and 4.3. In Figures 2 and 3, the experimentally detected acetaldehyde data are compared to the sum of the simulated mole fractions for acetaldehyde ethenol.

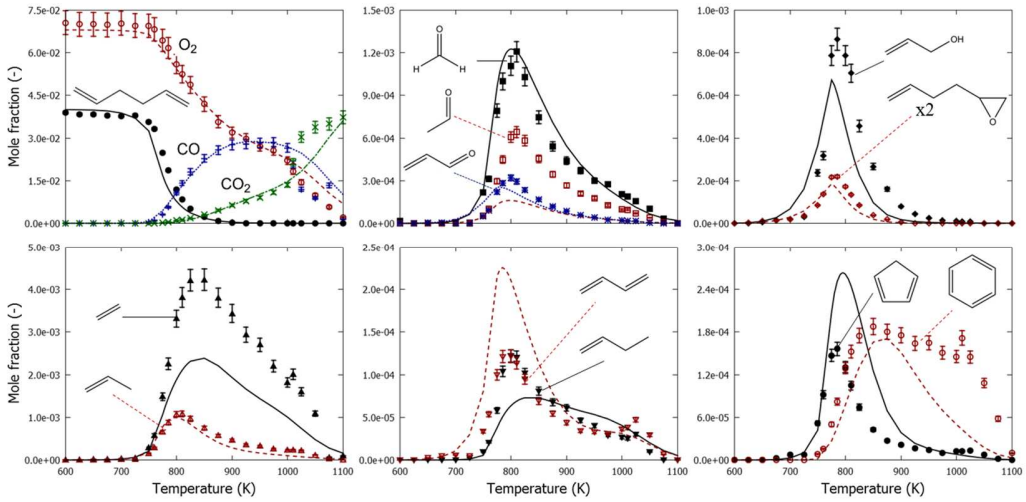

Figure 2: Mole fractions as function of temperature for 1,5-hexadiene oxidation in a jet-stirred reactor, P = 0.107 MPa, φ = 1.0, FV = 4.06 10^{-5} m^3 s^{-1}, $x_{1,5-hexadiene}^{inlet} = 0.008$: symbols, experimental mole fraction profile of molecule represented in graph; lines, mole fraction profiles calculated with CHEMKIN using the perfectly stirred reactor model and the developed kinetic model. For acetylene and 1,5-hexadiene experimental and model simulated mole fractions ×5 and for but-3-enyl-oxirane ×2.

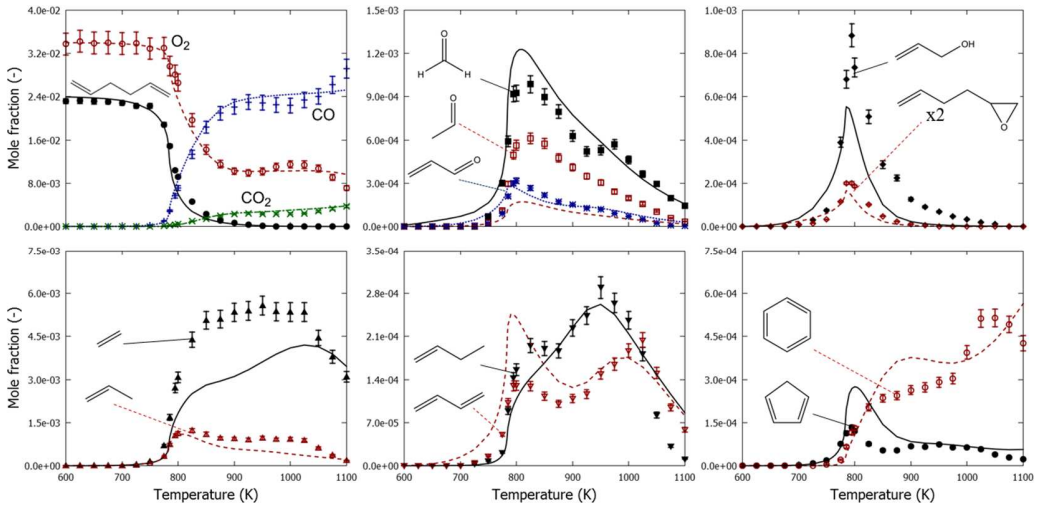

Figure 3: Mole fractions as function of temperature for 1,5-hexadiene oxidation in a jet-stirred reactor, P = 0.107 MPa, φ = 2.0, FV = 4.06 10^{-5} m^3 s^{-1}, $x_{1,5-hexadiene}^{inlet} = 0.008$: symbols, experimental mole fraction profile of molecule represented in graph; lines, mole fraction profiles calculated with CHEMKIN using the perfectly stirred reactor model and the developed kinetic model. For acetylene experimental and model simulated mole fraction ×5, for 1,5-hexadiene × 3 and for but-3-enyl-oxirane × 2.

The performance of the kinetic model for the pyrolysis of 1,5-hexadiene has been compared to the performance of the model developed by Wang et al. [6] for the pyrolysis of propene. The comparison of the performance for both kinetic models is added to the Supplementary Data. Although the model developed by Wang et al. [6] is developed for the pyrolysis of propene, it predicts the mole fractions of the small molecules formed in 1,5-hexadiene pyrolysis well. However, the current model performs better for the mole fractions of heavier, cyclic and aromatic species.

4.2. Primary decomposition pathways of 1,5-hexadiene

1,5-hexadiene is consumed by hydrogen abstraction, radical addition to the C-C double bonds and C-C scission. The importance of each consumption path depends on temperature and equivalence ratio. Reaction path analyses were performed at 800 K and 1000 K at $\varphi = 2.0$ and the results are presented in Figure 4.

Unimolecular decomposition of 1,5-hexadiene by C-C scission is fast and forms two allyl radicals. At low temperature and conversion, the allyl radicals are relatively unreactive and mainly recombine to 1,5-hexadiene. Thus 1,5-hexadiene and the allyl radicals are in thermodynamic equilibrium. At higher temperatures, 1,5-hexadiene and allyl radical concentrations deviate from equilibrium due to the faster consumption of allyl radicals compared to recombination of these radicals. In fuel-rich oxidation, C-C scission accounts for only 4% of the total 1,5-hexadiene consumption at 800 K, while it accounts for 92% of the total 1,5-hexadiene consumption at 1000 K.

Radicals can add to the terminal and the non-terminal carbon-atom of the C-C double bonds. Hydrogen atoms, hydroxyl radicals and methyl radicals are the main adding radicals at the investigated operating conditions. The addition of methyl radicals to the double bond is not shown in Figure 4. As it accounts for only 0.5% of the conversion at 800 K and $\varphi = 2.0$. Addition to the terminal carbon-atom of the CC double bond forms a secondary radical which can decompose by C-C β-scission forming an allyl radical and an unsaturated species, e.g. propene, prop-2-en-1-ol, 1-butene in the case of hydrogen atom, hydroxyl radical, methyl radical addition, respectively. Addition to the non-terminal carbon-atom of the C-C double bond forms a primary radical. C-C β-scission of the primary radical is in competition with intramolecular hydrogen abstraction through a five-membered transition state forming a resonantly stabilized radical, exo-intramolecular radical addition forming a five-membered ring and endo-intramolecular radical addition forming a six-membered ring. In the

case of hydrogen atom addition, these pathways may lead to ethene plus but-1-en-4-yl radical, 1,3-butadiene plus ethyl radical, cyclopentane-carbinyl radical and cyclohexyl radical as indicated in Figure 4.

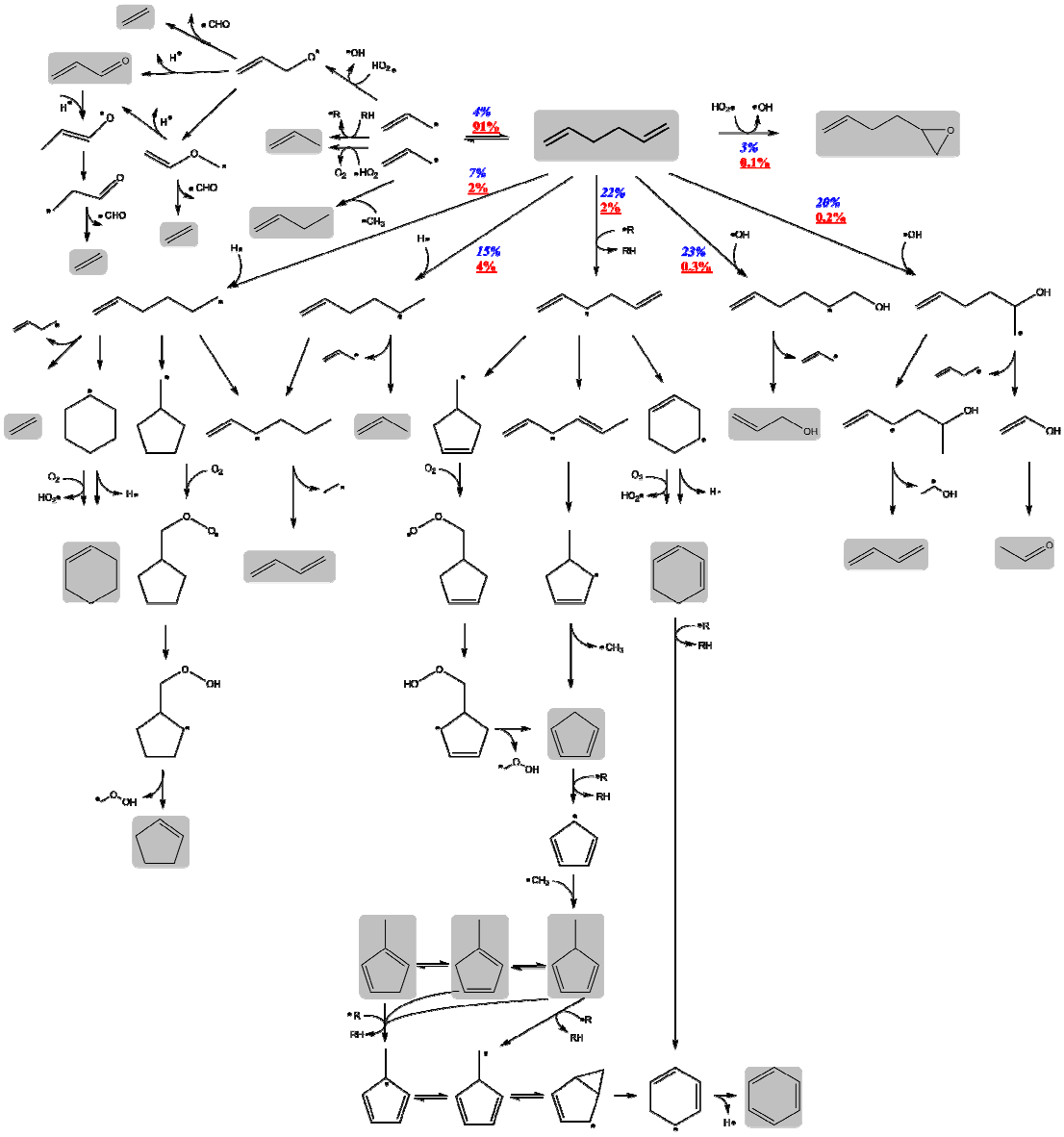

Figure 4: Reaction path analysis for 1,5-hexadiene consumption at fuel rich oxidizing conditions. Operating conditions: FV = 4.06 10^{-5} m^3 s^{-1}, $x_{1,5-hexadiene}^{inlet} = 0.008$, φ = 2.0, T = 800 K (blue and italic) and 1000 K (red and underlined). Percentages on a reaction path represent the reaction rate relative to the total 1,5-hexadiene decomposition rate. Species with a shaded background have been detected experimentally. (For interpretation of the references to colour in this figure legend, the reader is referred to the web version of this article.)

In the case of hydroxyl radical addition, C-C β-scission of the primary radical forms ethenol plus but-1-en-4-yl radical and intramolecular hydrogen abstraction followed by C-C β-scission forms 1-hydoxy-ethyl radical plus 1,3-butadiene, see Figure 4. Oxidation of 1-hydroxy-ethyl radical is the main acetaldehyde forming channel at 800 K. re-evaluation of the thermodynamic and kinetic parameters for the addition of hydroxyl radical to 1,5-hexadiene could potentially improve the sum of the acetaldehyde and ethenol predictions. Addition of hydroperoxy radical to the CC double bond and decomposition to cyclic ether leads to but-3-enyl-oxirane plus hydroxyl radical and is aminor pathway at low temperatures.

Hydrogen abstraction from the allylic carbon atom in 1,5-hexadiene forms the hexa-2,5-dien-1-yl radical. Hydrogen atom abstractions from the vinylic carbon atoms in 1,5-hexadiene are a minor pathway at the investigated conditions. These reactions account for only 3% of the conversion at 800 K and $\varphi = 2.0$. For this reason they omitted in Figure 4 and this discussion. The most important hydrogen abstracting species at 800 K and $\varphi = 2.0$ are hydroxyl radicals, hydrogen atoms and molecular oxygen. Abstractions by these species account for 62%, 11% and 12% of abstractions by all species respectively. At 1000 K, only 2% of 1,5-hexadiene is consumed by hydrogen abstraction reactions. At this temperature, hydrogen atom abstraction by hydrogen atoms accounts for 47% of all abstraction reactions, methyl radicals contribute to 22% and hydroxyl radicals to 18%. The formed hexa-2,5-dien-1-yl radical mainly reacts by intramolecular radical addition and intramolecular hydrogen abstraction at the investigated operating conditions. Recombination of hexa-2,5-dien-1-yl with hydroperoxy radical and reaction of hexa-2,5-dien-1-yl radicals with molecular oxygen forming 1,3,5-hexatriene and hydroperoxy radical were found to be unimportant. Intramolecular hydrogen abstraction of hexa-2,5-dien-1-yl radical forms hexa-2,4-dien-1-yl radical. Exo-intramolecular radical addition produces 5-methyl cyclopent-2-enyl, which after releasing methyl radicals in a subsequent β-scission form to 1,3-cyclopentadiene. Intramolecular radical addition of hexa-2,5-dien-1-yl radical through a five-membered transition state forms a cyclopentene-4-carbinyl radical. Consumption pathways of the latter radical to 4-methyl-cyclopentene-3-yl radical or to methylene-cyclopentene plus a hydrogen atom have relatively high energy barriers. Cyclopentene-4-carbinyl and hexa-2,5-dien-1-yl radicals are in quasi-equilibrium at low temperature pyrolysis conditions. In oxidation conditions, molecular oxygen can add on cyclopentene-4-carbinyl radical. According to the current model, the dominant reaction path of the adduct is intramolecular hydrogen abstraction from the allylic carbon atom and subsequent β-scission of the side group, which leads to 1,3-cyclopentadiene plus hydroperoxy-methyl radical, see Figure 4. Endo-intramolecular radical addition of hexa-2,5-

dien-1-yl forms cyclohexene-4-yl radical. CH β-scission of cyclohexene-4-yl radical forms 1,3-cyclohexadiene and 1,4-cyclohexadiene. The latter two molecules can also be formed through reaction of cyclohexene-4-yl radical with molecular oxygen.

Although often a major precursor for benzene, propargyl radicals are not present in Figure 4. The focus of this paragraph is on the primary decomposition products of 1,5-hexadiene and the subsequent formation of aromatics. Propargyl radicals are, at the experimental conditions used in this work, mainly formed by hydrogen abstraction reactions from propadiene and propyne. This secondary chemistry is not the focus of Figure 4.

Sensitivity analyses were performed to better understand the effect of the aforementioned reactions on the 1,5-hexadiene mole fraction profile. In the presented sensitivity analyses, a positive sensitivity coefficient for a given reaction indicates that increasing the associated pre-exponential factor increases the mole fraction of the target molecule. Analogously, a negative sensitivity coefficient for a given reaction indicates that increasing the associated pre-exponential factor decreases the mole fraction of the target molecule.

The sensitivity analysis with respect to 1,5-hexadiene mole fraction profile for pyrolysis conditions is displayed in Figure 5. The conversion of 1,5-hexadiene in pyrolysis is very sensitive towards hydrogen abstraction by allyl radicals from 1,5-hexadiene, with a significant promoting effect on reactivity. Also hydrogen abstractions by hydrogen atoms and methyl radicals from 1,5-hexadiene have negative sensitivity coefficients. The sensitivity analysis indicates the importance of allyl radicals during the pyrolysis of 1,5-hexadiene. Except for the hydrogen abstraction by allyl radicals from 1,5-hexadiene, almost all reactions that consume allyl radicals have a negative sensitivity coefficients and almost all reactions in which allyl radicals are formed have a positive sensitivity coefficient.

Allyl radicals formed through these reactions influence the equilibrium between 1,5-hexadiene and allyl radicals, hence increasing the 1,5-hexadiene mole fraction. Hydrogen addition to the CC double bond forming hex-5-en-2-yl radical has a positive sensitivity coefficient as hex-5-en-2-yl radical mainly decomposes to an allyl radical while hydrogen addition to the CC double bond forming hex-5-en-1-yl has a negative sensitivity coefficient as decomposition of hex-5-en-1-yl radicals mainly results in reactive hydrogen atoms.

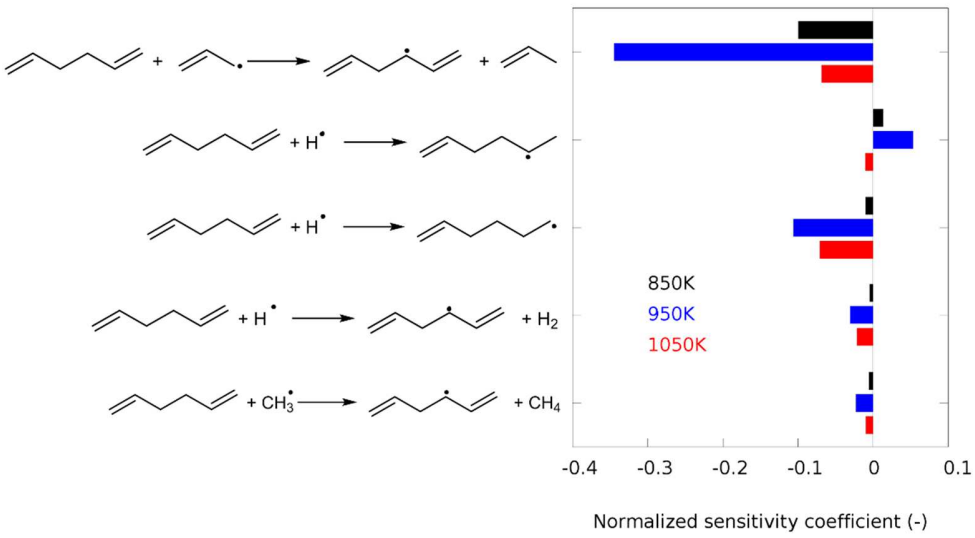

Figure 5: Sensitivity coefficients for 1,5-hexadiene mole fraction in 1,5-hexadiene pyrolysis. Operating conditions correspond to P = 0.107 MPa, FV = 4.06 10^{-5} m^3 s^{-1}, $x_{1,5-hexadiene}^{inlet} = 0.008$, T = 850 K (black), 950 K (red), and 1050 K (blue). (For interpretation of the references to colour in this figure legend, the reader is referred to the web version of this article.)

The sensitivity analysis with respect to 1,5-hexadiene mole fraction profile for fuel-rich oxidations conditions at T = 750 K, 850 K, 950 K and 1050 K is displayed in Figure 6.

At the lowest temperatures, the 1,5-hexadiene mole fraction is sensitive to reactions involved in the primary 1,5-hexadiene consumption. Similar to pyrolysis, these include hydrogen abstraction reactions to form hex-1,5-dien-3-yl radical and addition to the C-C double bounds. In fuel-rich oxidation conditions, the 1,5-hexadiene mole fraction is most sensitive to hydrogen abstractions by molecular oxygen and hydroxyl radicals and to addition of hydrogen atoms and hydroxyl radicals. Most of these reactions have a negative sensitivity coefficient as they contribute to the consumption of 1,5-hexadiene. Positive sensitivity coefficients for the addition of hydrogen atoms and hydroxyl radicals to the C-C double bond, with the formation of hex-5-en-2-yl and hex-5-en-1-ol-2-yl respectively, are caused by the formation of allyl radicals during the decomposition of these radicals. This is reasonable since allyl radicals formation increases 1,5-hexadiene concentration through the recombination reaction.

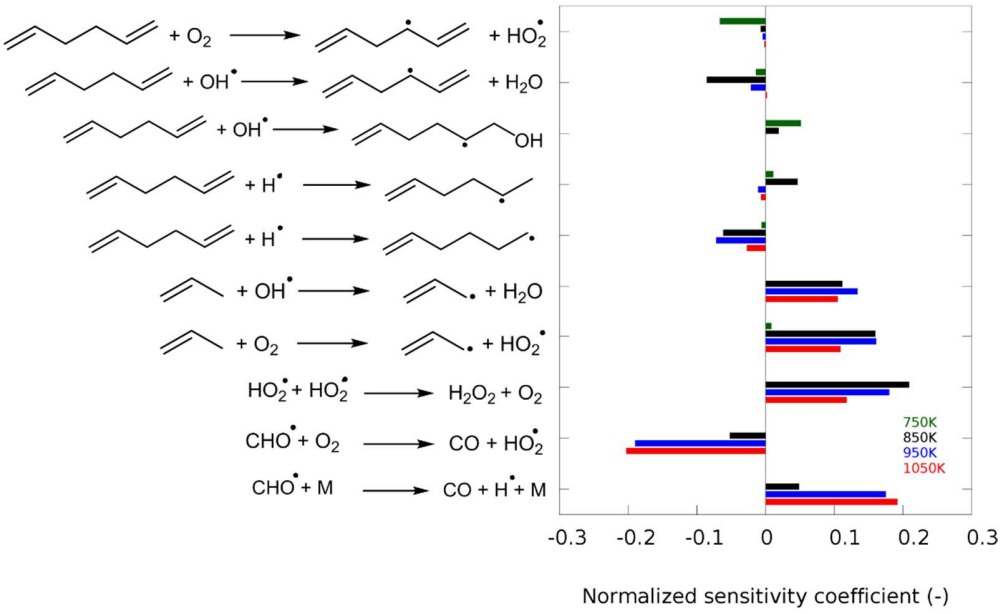

Figure 6: Sensitivity coefficients for 1,5-hexadiene mole fraction in 1,5-hexadiene oxidation. Operating conditions correspond to P = 0.107 MPa, φ = 2.0, FV = 4.06 10^{-5} m^3 s^{-1}, $x_{1,5-hexadiene}^{inlet}$ = 0.008, T = 750 K (green), 850 K (black), 950 K (blue) and 1050 K (red). (For interpretation of the references to colour in this figure legend, the reader is referred to the web version of this article.)

At higher oxidation temperatures, the 1,5-hexadiene mole fraction is more sensitive to reactions that are part of the secondary combustion chemistry. Hydrogen abstraction from propene by molecular oxygen has a positive sensitivity coefficient. Although this reaction increases the number of radicals in the reactive system, allyl radicals are formed, influencing the equilibrium and hence increasing the 1,5-hexadiene mole fraction. Self-reaction of hydroperoxy radicals giving hydrogen peroxide plus molecular oxygen has a positive sensitivity coefficient as this results in a net decrease of radicals in the system. Moreover, hydroperoxy radicals are involved in the main allyl radical consumption pathways, as can be seen in Figure 4 and explained more detailed in section 4.3. A decrease in the number of hydroperoxy radicals decreases the reactivity of the allyl radicals through these pathways. Because of the equilibrium between 1,5-hexadiene and allyl radicals, an increase in 1,5-hexadiene mole fraction is expected. The negative sensitivity coefficient for the reaction of formyl radical with molecular oxygen to carbon monoxide and hydroxyperoxy radical can also be explained by the involvement of the hydroperoxy radicals in the allyl radical consumption pathways. The competing decomposition of formyl radical to carbon monoxide and a reactive hydrogen radical has a positive

sensitivity coefficient. A sensitivity analysis with respect to the allyl radical mole fraction is provided in the Supplementary Material.

4.3. Allyl reaction pathways

The allyl radical, which is formed in large quantities, has several consumption pathways including abstraction reactions forming propene and recombination reactions with hydrogen atoms or radicals. C-H β-scission to allene plus hydrogen atom is a minor allyl consumption pathway, similar to the oxidation of propene at comparable operating conditions [29].

The recombination of allyl with methyl radical is a significant pathway in fuel-rich oxidation and pyrolysis conditions. At 1000 K and $\varphi = 2.0$, this is the dominant 1-butene formation pathway. Note that this recombination reaction is part of the Burke propene oxidation mechanism [29,30] and reaction rate coefficients are taken from Kynazev and Slagle [61]. Subsequent consumption of 1-butene by hydrogen abstraction and C-H β-scission leads to 1,3-butadiene[62] and is the cause of the experimentally observed second maximum in the 1,3-butadiene yield at 1000 K shown in Figure 3.

At oxidizing conditions, an important pathway for allyl radicals is the reaction with the hydroperoxy radical, in which allyloxy and hydroxyl radicals are formed, as can be seen in Figure 4. The potential energy surface of the allyloxy radical, that is included in the Burke propene oxidation mechanism [29,30], is calculated theoretically by Goldsmith et al. [52]. The main pathways include the C-H β-scission forming acrolein and a hydrogen atom, the formation of ethene and a formyl radical and the unimolecular formation of vinyloxymethyl radical. These reaction pathways and the relative concentrations of the C_3H_5O radicals, i.e. allyloxy, 3-oxo-propyl, 2-oxo-propyl and vinyloxymethyl radical, are important for accurate predictions of the observed product spectrum. C-H β-scissions of these radicals are the dominant acrolein formation paths at the investigated conditions. The decomposition of the C_3H_5O radicals to formyl radicals and ethene contributes for more than 50% to the total ethene production at 800 K and $\varphi = 2.0$. Re-evaluation of the branching ratio of the competing reactions can help to improve the agreement between model and experiment and is suggested for further studies. The recombination of allyl with hydroperoxy radicals competes with hydrogen atom abstraction from hydroperoxy by allyl.

4.4. Formation of aromatics

Benzene is the most abundant aromatic compound in the oxidation and pyrolysis of 1,5-hexadiene. Cyclohexadiene and 1,3-cyclopentadiene are important benzene precursors. Cyclohexadiene yields benzene after hydrogen abstraction and subsequent C-H β-scission. Direct elimination of molecular hydrogen from 1,3-cyclohexadiene and 1,4-cyclohexadiene proceeds through high barriers. These reactions are negligible for benzene formation at the experimental conditions of this study. Cyclopentadienyl contributes to benzene formation through the recombination reaction with methyl radical. Hydrogen abstraction from methyl-cyclopentadiene followed by ring enlargement gives eventually benzene, as indicated in Figure 4. This pathway has been extensively discussed in the past [6,10,17].

As mentioned earlier, the benzene precursors cyclohexadiene and 1,3-cyclopentadiene are formed from the hexa-2,5-dien-1-yl radical. This radical is produced by hydrogen abstraction from the fuel and by addition of vinyl to 1,3-butadiene. At fuel-rich conditions ($\varphi = 2.0$), the former pathway to hexa-2,5-dien-1-yl radical is more important below 900 K while the latter pathway dominates above 900 K. A different route to 1,3-cyclopentadiene at high temperature is the addition of allyl to ethene, followed by intramolecular radical addition and dehydrogenation reactions. The addition of allyl radicals to ethyne also produces 1,3-cyclopentadiene after intramolecular addition and dehydrogenation reactions.

At oxidation conditions, the pathways to benzene and 1,3-cyclopentadiene that are related to the decomposition of the feed molecular structure give rise to the first peak of the benzene yield while the pathways related to reactions of small molecules, such as vinyl, allyl, ethene, ethyne, propargyl and 1,3-butadiene give rise to the second peak in the benzene yield, see Figure 3. This is reflected in the sensitivity analysis for benzene and 1,3-cyclopentadiene production in fuel-rich oxidation, displayed in Figures 7 and 8, respectively. The 1,3-cyclopentadiene and benzene mole fraction profiles are sensitive to reactions that have an effect on 1,5-hexadiene conversion, discussed in section 4.2. Also reactions that are important for the formation of benzene and 1,3-cyclopentadiene starting from the fuel structure, e.g. intramolecular radical addition of hexa-2,5-dien-1-yl to cyclohexene-4-yl radical, and reactions involved in the direct consumption of the benzene and 1,3-cyclopentadiene have high sensitivity coefficients. At the highest temperatures, other reactions involved in the secondary oxidation chemistry, have an increased importance, as presented in Figures

7 and 8. Benzene mole fraction profiles are sensitive to the recombination of 1,3-cyclopentadienyl radical with methyl radicals, the initial reaction in a second pathway for the production of benzene, see Figure 4. 1,3-cyclopentadiene mole fractions are sensitive to the formation of 1-butene by the recombination of allyl and methyl radicals and to the formation of ethene and vinyl radicals after β-scission of but-1-en-4-yl radicals. The addition of allyl radicals to acetylene, forming penta-1,3-dien-5-yl, is a sensitive reaction for both benzene and 1,3-cyclopentadiene mole fractions.

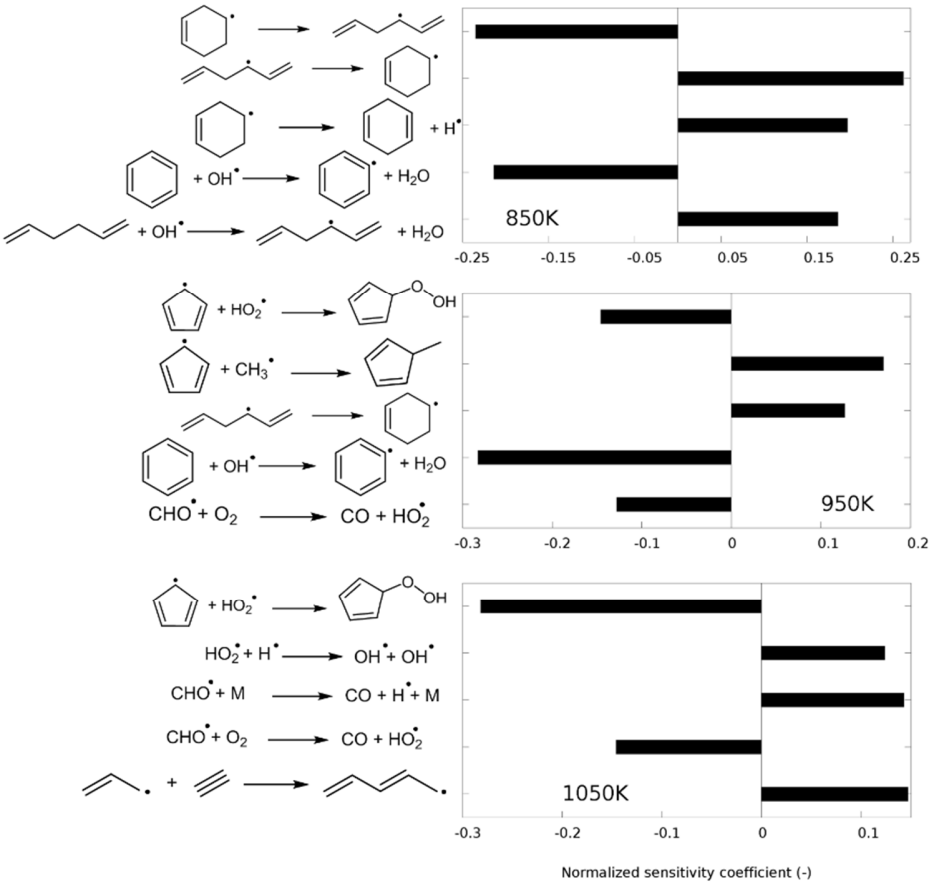

Figure 7: Sensitivity coefficients for benzene mole fraction in 1,5-hexadiene oxidation. Operating conditions correspond to P = 0.107 MPa, φ = 2.0, FV = 4.06 10^{-5} m^3 s^{-1}, $x_{1,5-hexadiene}^{inlet} = 0.008$, T = 850 K, 950 K and 1050 K.

Also the recombination reaction between propargyl radicals and allyl radicals is an important pathway for the formation of benzene. Through this reaction, hex-1-en-5-yne or 1,2,5-hexatriene can be formed. 1,2,5-hexatriene mainly undergoes an isomerization reaction to form hex-1-en-5-yne.

After cyclization with the loss of a hydrogen atom and several isomerizations, methyl-2,4-cyclopentadien-1-yl is formed. As can be seen in Figure 4, methyl-2,4-cyclopentadien-1-yl easily converts to benzene. At $\varphi = 2.0$ and 1000 K, the recombination of allyl and propargyl radicals is responsible for 21% of the total benzene production. The importance of this reaction increases with increasing temperature. Some reactions related to the propargyl radical are sensitive reactions for the benzene mole fraction. These include for example the hydrogen abstraction reaction by hydrogen atoms from propadiene and propyne and the cyclization of hex-1-en-5-yne with the loss of a hydrogen atom. The normalized sensitivity coefficients for these reactions are however much smaller compared to the ones reported in Figure 7. For this reason, they are not shown.

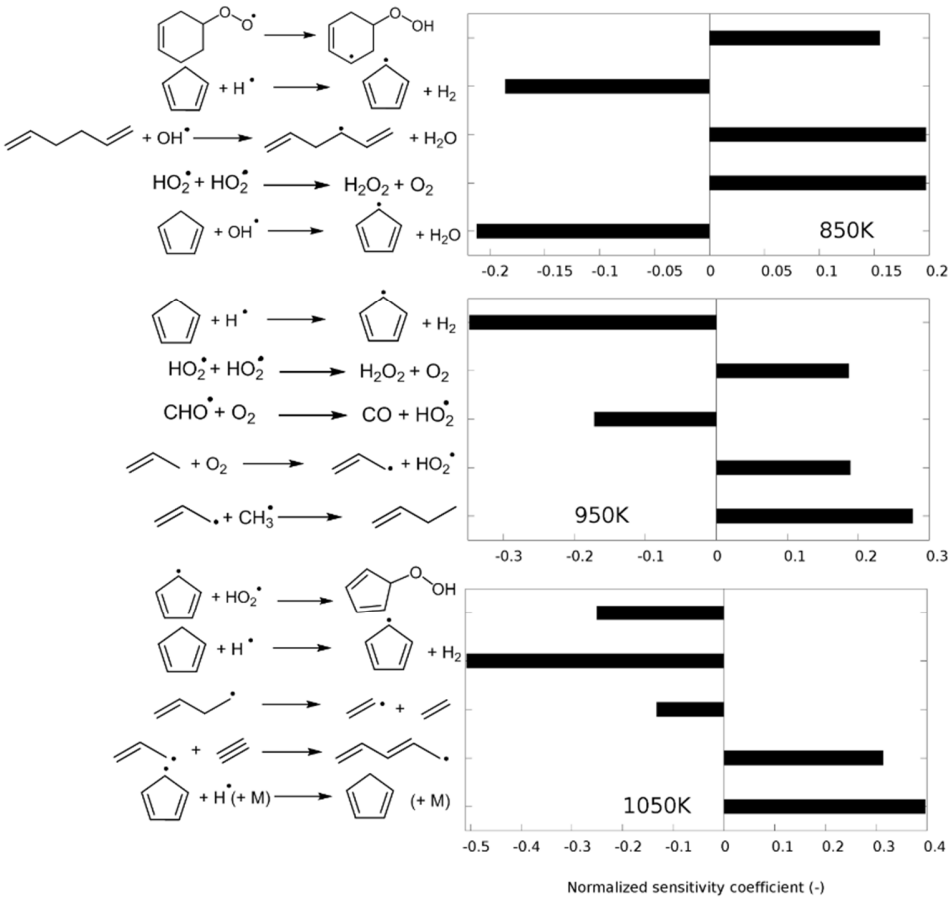

Figure 8: Sensitivity coefficients for 1,3-cyclopentadiene mole fraction in 1,5-hexadiene oxidation. Operating conditions correspond to P = 0.107 MPa, $\varphi = 2.0$, FV = 4.06 10^{-5} m^3 s^{-1}, $x_{1,5-hexadiene}^{inlet} = 0.008$, T = 850 K, 950 K and 1050 K.

Several other aromatics were detected in the reactor outlet gases, e.g. toluene, styrene, indene and naphthalene. Especially at pyrolysis conditions, they have relatively high yields. The pathways to substituted aromatics, such as toluene and styrene, are similar to the discussed benzene pathways (see Figure 9). Toluene is mainly formed by recombination of allyl with but-1-en-3-yl followed by hydrogen abstraction and intramolecular radical addition reaction, analogous to the formation of benzene starting from 1,5-hexadiene. A second route to toluene is the recombination of ethyl with 1,3-cyclopentadienyl, followed by hydrogen abstraction and ring enlargement, analogous to the formation of benzene starting from the recombination of methyl with 1,3-cyclopentadienyl radical. Recombination of allyl with 1,3-cyclopentadienyl radicals is the dominant path to styrene. The subsequent reaction sequence is, again, analogous to methyl plus 1,3-cyclopentadienyl radical giving benzene.

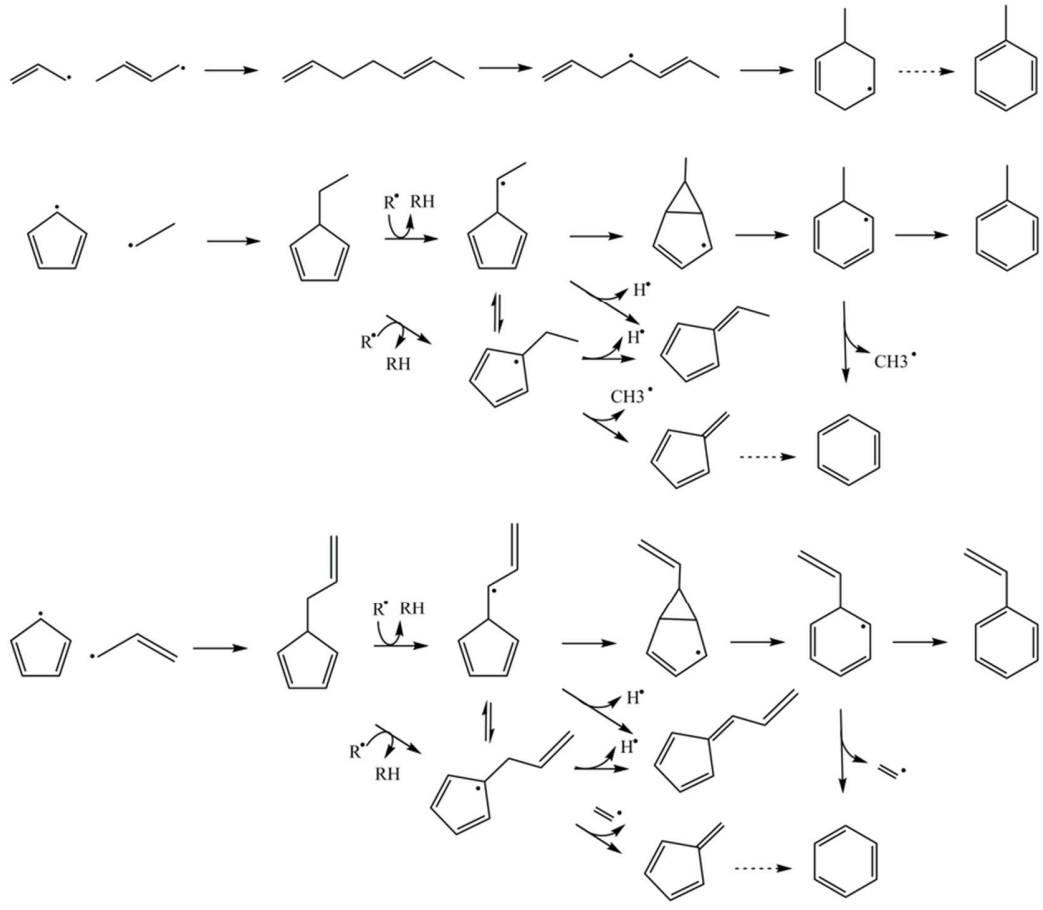

Figure 9: Formation of aromatics in the pyrolysis of 1,5-hexadiene starting from initial decomposition products of 1,5-hexadiene. Reactions involving propargyl radicals are not included.

5. Conclusions

1,5-hexadiene is an excellent molecule to study the role of allylic radicals in the formation of aromatic molecules. Therefore, oxidation and pyrolysis experiments were performed in a jet-stirred reactor, below 1100 K. The experimental data is supported by a new detailed kinetic model, which was developed using a combination of the Burke propene oxidation mechanism [29,30], automatic network generation and literature-reported quantum chemical calculations. Without any adjustments, the model describes all experimental data qualitatively well, but for some compounds, such as ethene, acrolein and acetaldehyde, quantitative differences exist, especially in the presence of oxygen. At the investigated operating conditions, the reactor effluent composition is sensitive towards reactions involving allyl radicals, e.g. hydrogen abstraction from 1,5-hexadiene by allyl radical and its reaction with hydroperoxy radical. The pyrolysis and oxidation of 1,5-hexadiene has a high selectivity to benzene. It can be formed by intramolecular addition of the hexa-2,5-dien-1-yl radical, which is formed by hydrogen abstraction from 1,5-hexadiene, or alternatively by a reaction sequence that starts with the recombination of cyclopentadienyl and methyl radicals. The pathways responsible for benzene formation can be extrapolated to substituted aromatics such as toluene and styrene

Acknowledgments

The authors acknowledge the financial support from the Long Term Structural Methusalem Funding by the Flemish Government, the European Research Council (ERC) under the European Union's Seventh Framework Program (FP7/2007-2013)/ERC grant agreement n° 290793, the Research Board of Ghent University (BOF), the Fund for Scientific Research Flanders (FWO) and the COST Action CM1404 "Chemistry of smart energy carriers and technologies". The SBO proposals "Bioleum" and "Arboref" supported by the Institute for promotion of Innovation through Science and Technology in Flanders (IWT) are acknowledged.

Supplementary Material

Experimental data of the pyrolysis and oxidation of 1,5-hexadiene in a jet-stirred reactor ($\varphi = \infty$,1.0 and 2.0)

Kinetic model for the oxidation and pyrolysis of 1,5-hexadiene

Reaction families in Genesys to construct the 1,5-hexadiene submechanism

References

[1] H. Richter, J.B. Howard, Formation of polycyclic aromatic hydrocarbons and their growth to soot - a review of chemical reaction pathways, Prog. Energy Combust. Sci., 26 (2000) 565-608.

[2] N. Hansen, W. Li, M.E. Law, T. Kasper, P.R. Westmoreland, B. Yang, T.A. Cool, A. Lucassen, The importance of fuel dissociation and propargyl + allyl association for the formation of benzene in a fuel-rich 1-hexene flame, Phys. Chem. Chem. Phys., 12 (2010) 12112-12122.

[3] M.R. Djokic, K.M. Van Geem, C. Cavallotti, A. Frassoldati, E. Ranzi, G.B. Marin, An experimental and kinetic modeling study of cyclopentadiene pyrolysis: First growth of polycyclic aromatic hydrocarbons, Combust. Flame, 161 (2014) 2739-2751.

[4] J.A. Miller, M.J. Pilling, J. Troe, Unravelling combustion mechanisms through a quantitative understanding of elementary reactions, P. Combust. Inst., 30 (2005) 43-88.

[5] J.A. Miller, C.F. Melius, Kinetic and thermodynamic issues in the formation of aromatic compounds in flames of aliphatic fuels, Combust. Flame, 91 (1992) 21-39.

[6] K. Wang, S.M. Villano, A.M. Dean, Fundamentally-based kinetic model for propene pyrolysis, Combust. Flame, 162 (2015) 4456-4470.

[7] Y. Georgievskii, J.A. Miller, S.J. Klippenstein, Association rate constants for reactions between resonance-stabilized radicals: C3H3 + C3H3, C3H3 + C3H5, and C3H5 + C3H5, Phys. Chem. Chem. Phys., 9 (2007) 4259-4268.

[8] N. Hansen, J.A. Miller, P.R. Westmoreland, T. Kasper, K. Kohse-Höinghaus, J. Wang, T.A. Cool, Isomer-specific combustion chemistry in allene and propyne flames, Combust. Flame, 156 (2009) 2153-2164.

[9] N. Hansen, T. Kasper, B. Yang, T.A. Cool, W. Li, P.R. Westmoreland, P. Oßwald, K. Kohse-Höinghaus, Fuel-structure dependence of benzene formation processes in premixed flames fueled by C6H12 isomers, P. Combust. Inst., 33 (2011) 585-592.

[10] E. Ikeda, R.S. Tranter, J.H. Kiefer, R.D. Kern, H.J. Singh, Q. Zhang, The pyrolysis of methylcyclopentadiene: Isomerization and formation of aromatics, P. Combust. Inst., 28 (2000) 1725-1732.
[11] A. Nawdiyal, N. Hansen, T. Zeuch, L. Seidel, F. Mauß, Experimental and modelling study of speciation and benzene formation pathways in premixed 1-hexene flames, P. Combust. Inst., 35 (2015) 325-332.
[12] X. Fu, X. Han, K. Brezinsky, S. Aggarwal, Effect of Fuel Molecular Structure and Premixing on Soot Emissions from n-Heptane and 1-Heptene Flames, Energ. Fuel., 27 (2013) 6262-6272.
[13] Z.J. Buras, E.E. Dames, S.S. Merchant, G. Liu, R.M.I. Elsamra, W.H. Green, Kinetics and Products of Vinyl + 1,3-Butadiene, a Potential Route to Benzene, J. Phys. Chem. A, 119 (2015) 7325-7338.
[14] P. Barbé, R. Martin, D. Perrin, G. Scacchi, Kinetics and modeling of the thermal reaction of propene at 800 K. Part I. Pure propene, Int. J. Chem. Kinet., 28 (1996) 829-847.
[15] R. De Bruycker, H.-H. Carstensen, M.-F. Reyniers, G.B. Marin, J.M. Simmie, K.M. Van Geem, An experimental and kinetic modeling study of γ-valerolactone pyrolysis, Combust. Flame, 164 (2016) 183-200.
[16] K. Wang, S.M. Villano, A.M. Dean, Reactions of allylic radicals that impact molecular weight growth kinetics, Phys. Chem. Chem. Phys., 17 (2015) 6255-6273.
[17] S. Sharma, M.R. Harper, W.H. Green, Modeling of 1,3-hexadiene, 2,4-hexadiene and 1,4-hexadiene-doped methane flames: Flame modeling, benzene and styrene formation, Combust. Flame, 157 (2010) 1331-1345.
[18] D.J. Ruzicka, W.A. Bryce, The pyrolysis of diallyl (1,5-hexadiene), Canadian Journal of Chemistry, 38 (1960) 827-834.
[19] D.M. Golden, N.A. Gac, S.W. Benson, Direct measurement of allyl resonance energy. Equilibrium constant for allyl radical recombination, Abstr. Pap. Am. Chem. Soc., (1969) PH50-&.
[20] J.B. Homer, F.P. Lossing, Free radicals by mass spectrometry. 35. Heat of formation of allyl radical from biallyl pyrolysis, Canadian Journal of Chemistry, 44 (1966) 2211-&.
[21] R.J. Akers, Throssel.Jj, Kinetic studies on allyl radicals. 1. Toluene-carrier pyrolysis of 4-phenyl-but-1-ene and hexa-1,5-diene and heat of formation of allyl radical, Transactions of the Faraday Society, 63 (1967) 124-&.
[22] D. Nohara, T. Sakai, Thermal Reaction of 1,5-Hexadiene. Mechanism Proposal, Product R&D, 12 (1973) 322-325.

[23] J.K. McDonald, J.A. Merritt, B.J. Alley, S.P. McManus, Gas-phase thermolysis of 1,5-hexadiene: the continuous wave carbon dioxide laser-induced reaction and studies of the cyclization pathway, J. Am. Chem. Soc., 107 (1985) 3008-3012.
[24] S.J. Isemer, K. Luther, Shock tube studies on the high temperature chemical kinetics of allyl radicals: reactions with C2H2, CH4, H-2 and C3H5 at 1000-1400 K, Springer-Verlag Berlin, Berlin, 2005.
[25] A. Matsugi, K. Suma, A. Miyoshi, Kinetics and Mechanisms of the Allyl + Allyl and Allyl + Propargyl Recombination Reactions, The Journal of Physical Chemistry A, 115 (2011) 7610-7624.
[26] A. Fridlyand, P.T. Lynch, R.S. Tranter, K. Brezinsky, Single Pulse Shock Tube Study of Allyl Radical Recombination, J. Phys. Chem. A, 117 (2013) 4762-4776.
[27] Y. Georgievskii, J.A. Miller, S.J. Klippenstein, Association rate constants for reactions between resonance-stabilized radicals: C3H3+C3H3, C3H3+C3H5, and C3H5+C3H5, Phys. Chem. Chem. Phys., 9 (2007) 4259-4268.
[28] C.S. McEnally, L.D. Pfefferle, Decomposition and hydrocarbon growth processes for hexadienes in nonpremixed flames, Combust. Flame, 152 (2008) 469-481.
[29] S.M. Burke, W. Metcalfe, O. Herbinet, F. Battin-Leclerc, F.M. Haas, J. Santner, F.L. Dryer, H.J. Curran, An experimental and modeling study of propene oxidation. Part 1: Speciation measurements in jet-stirred and flow reactors, Combust. Flame, 161 (2014) 2765-2784.
[30] S.M. Burke, U. Burke, R. Mc Donagh, O. Mathieu, I. Osorio, C. Keesee, A. Morones, E.L. Petersen, W.J. Wang, T.A. DeVerter, M.A. Oehlschlaeger, B. Rhodes, R.K. Hanson, D.F. Davidson, B.W. Weber, C.J. Sung, J. Santner, Y.G. Ju, F.M. Haas, F.L. Dryer, E.N. Volkov, E.J.K. Nilsson, A.A. Konnov, M. Alrefae, F. Khaled, A. Farooq, P. Dirrenberger, P.A. Glaude, F. Battin-Leclerc, H.J. Curran, An experimental and modeling study of propene oxidation. Part 2: Ignition delay time and flame speed measurements, Combust. Flame, 162 (2015) 296-314.
[31] O. Herbinet, F. Battin-Leclerc, Progress in Understanding Low-Temperature Organic Compound Oxidation Using a Jet-Stirred Reactor, Int. J. Chem. Kinet., 46 (2014) 619-639.
[32] O. Herbinet, B. Sirjean, F. Battin-Leclerc, R. Fournet, P.-M. Marquaire, Thermal Decomposition of Norbornane (bicyclo[2.2.1]heptane) Dissolved in Benzene: Experimental Study and Mechanism Investigation, Energ. Fuel., 21 (2007) 1406-1414.
[33] O. Herbinet, Etude expérimentale et modélisation de la décomposition thermique de l'exo-tricyclo [5. 2. 1. 0 2,6] décane, in: Thèse de doctorat Génie des procédés et des produits, Vandoeuvre-les-Nancy, INPL, 2006, pp. 1 vol. (228 p.).

[34] L.S. Tran, Étude de la formation de polluants lors de la combustion de carburants oxygénés, in: Thèse de doctorat Génie des procédés et des produits, Université de Lorraine, 2013.
[35] R.J. Kee, F.M. Rupley, J.A. Miller, M.E. Coltrin, J.F. Grcar, E. Meeks, H.K. Moffat, A.E. Lutz, G. Dixon-Lewis, M.D. Smooke, J. Warnatz, G.H. Evans, L.R. S., R.E. Mitchell, L.R. Petzold, W.C. Reynolds, M. Caracotsios, W.E. Stewart, P. Glarborg, C. Wang, O. Adigun, CHEMKIN-PRO, in, Reaction Design, Inc., San Diego (CA), 2010.
[36] N.M. Vandewiele, K.M. Van Geem, M.-F. Reyniers, G.B. Marin, Genesys: Kinetic model construction using chemo-informatics, Chem. Eng. J., 207 (2012) 526-538.
[37] R. Van de Vijver, N.M. Vandewiele, P.L. Bhoorasingh, B.L. Slakman, F. Seyedzadeh Khanshan, H.-H. Carstensen, M.-F. Reyniers, G.B. Marin, R.H. West, K.M. Van Geem, Automatic Mechanism and Kinetic Model Generation for Gas- and Solution-Phase Processes: A Perspective on Best Practices, Recent Advances, and Future Challenges, International Journal of Chemical Kinetics, 47 (2015) 199-231.
[38] C.F. Goldsmith, G.R. Magoon, W.H. Green, Database of Small Molecule Thermochemistry for Combustion, J. Phys. Chem. A, 116 (2012) 9033-9057.
[39] E. Goos, A. Burcat, B. Ruscic, Extended Third Millennium Thermodynamic Database for Combustion and Air-Pollution Use with Updates from Active Thermochemical Tables, 2014.
[40] S.W. Benson, Thermochemical Kinetics: Methods for the Estimation of Thermochemical Data and Rate Parameters, John Wiley & Sons, New York, 1976.
[41] M. Saeys, M.F. Reyniers, G.B. Marin, V. Van Speybroeck, M. Waroquier, Ab initio group contribution method for activation energies for radical additions, Aiche J., 50 (2004) 426-444.
[42] M.K. Sabbe, M.F. Reyniers, V. Van Speybroeck, M. Waroquier, G.B. Marin, Carbon-centered radical addition and beta-scission reactions: Modeling of activation energies and pre-exponential factors, ChemPhysChem, 9 (2008) 124-140.
[43] M.K. Sabbe, M. Saeys, M.F. Reyniers, G.B. Marin, V. Van Speybroeck, M. Waroquier, Group additive values for the gas phase standard enthalpy of formation of hydrocarbons and hydrocarbon radicals, J. Phys. Chem. A, 109 (2005) 7466-7480.
[44] M.K. Sabbe, A.G. Vandeputte, M.F. Reyniers, M. Waroquier, G.B. Marin, Modeling the influence of resonance stabilization on the kinetics of hydrogen abstractions, Phys. Chem. Chem. Phys., 12 (2010) 1278-1298.
[45] R. Sivaramakrishnan, J.V. Michael, Rate Constants for OH with Selected Large Alkanes: Shock-Tube Measurements and an Improved Group Scheme, J. Phys. Chem. A, 113 (2009) 5047-5060.

[46] P.D. Paraskevas, M.K. Sabbe, M.-F. Reyniers, N.G. Papayannakos, G.B. Marin, Group Additive Kinetics for Hydrogen Transfer Between Oxygenates, J. Phys. Chem. A, (2015).
[47] J. Aguilera-Iparraguirre, H.J. Curran, W. Klopper, J.M. Simmie, Accurate Benchmark Calculation of the Reaction Barrier Height for Hydrogen Abstraction by the Hydroperoxyl Radical from Methane. Implications for CnH2n+2 where n = 2 → 4, J. Phys. Chem. A, 112 (2008) 7047-7054.
[48] J. Zádor, S.J. Klippenstein, J.A. Miller, Pressure-Dependent OH Yields in Alkene + HO2 Reactions: A Theoretical Study, J. Phys. Chem. A, 115 (2011) 10218-10225.
[49] K. Wang, S.M. Villano, A.M. Dean, Reactivity–Structure-Based Rate Estimation Rules for Alkyl Radical H Atom Shift and Alkenyl Radical Cycloaddition Reactions, J. Phys. Chem. A, 119 (2015) 7205-7221.
[50] J. Bugler, K.P. Somers, E.J. Silke, H.J. Curran, Revisiting the Kinetics and Thermodynamics of the Low-Temperature Oxidation Pathways of Alkanes: A Case Study of the Three Pentane Isomers, J. Phys. Chem. A, 119 (2015) 7510-7527.
[51] F. Zhang, T.S. Dibble, Effects of Olefin Group and Its Position on the Kinetics for Intramolecular H-Shift and HO2 Elimination of Alkenyl Peroxy Radicals, J. Phys. Chem. A, 115 (2011) 655-663.
[52] C.F. Goldsmith, S.J. Klippenstein, W.H. Green, Theoretical rate coefficients for allyl + HO2 and allyloxy decomposition, P. Combust. Inst., 33 (2011) 273-282.
[53] C.K. Westbrook, W.J. Pitz, M. Mehl, P.-A. Glaude, O. Herbinet, S. Bax, F. Battin-Leclerc, O. Mathieu, E.L. Petersen, J. Bugler, H.J. Curran, Experimental and Kinetic Modeling Study of 2-Methyl-2-Butene: Allylic Hydrocarbon Kinetics, J. Phys. Chem. A, 119 (2015) 7462-7480.
[54] P.T. Lynch, C.J. Annesley, C.J. Aul, X. Yang, R.S. Tranter, Recombination of Allyl Radicals in the High Temperature Fall-Off Regime, J. Phys. Chem. A, 117 (2013) 4750-4761.
[55] J.A. Miller, S.J. Klippenstein, Y. Georgievskii, L.B. Harding, W.D. Allen, A.C. Simmonett, Reactions between Resonance-Stabilized Radicals: Propargyl + Allyl, J. Phys. Chem. A, 114 (2010) 4881-4890.
[56] J.A. Miller, S.J. Klippenstein, The recombination of propargyl radicals and other reactions on a C6H6 potential, J. Phys. Chem. A, 107 (2003) 7783-7799.
[57] S.S. Merchant, Molecules to Engines: Combustion Chemistry of Alcohols and their Application to Advanced Engines, in, Massachusetts Institute of Technology, Massachusetts, United States, 2015.
[58] O. Herbinet, B. Husson, M. Ferrari, P.-A. Glaude, F. Battin-Leclerc, Low temperature oxidation of benzene and toluene in mixture with n-decane, P. Combust. Inst., 34 (2013) 297-305.
[59] J. Zádor, C.A. Taatjes, R.X. Fernandes, Kinetics of elementary reactions in low-temperature autoignition chemistry, Prog. Energy Combust. Sci., 37 (2011) 371-421.

[60] M. Pelucchi, M. Bissoli, C. Cavallotti, A. Cuoci, T. Faravelli, A. Frassoldati, E. Ranzi, A. Stagni, Improved Kinetic Model of the Low-Temperature Oxidation of n-Heptane, Energ. Fuel., 28 (2014) 7178-7193.
[61] V.D. Knyazev, I.R. Slagle, Kinetics of the Reactions of Allyl and Propargyl Radicals with CH3, J. Phys. Chem. A, 105 (2001) 3196-3204.
[62] Y. Fenard, G. Dayma, F. Halter, F. Foucher, Z. Serinyel, P. Dagaut, Experimental and Modeling Study of the Oxidation of 1-Butene and cis-2-Butene in a Jet-Stirred Reactor and a Combustion Vessel, Energ. Fuel., 29 (2015) 1107-1118.